Smart Structures and Systems, *Vol. 26, No. 5* (*2020*) *575-589*
DOI: https://doi.org/10.12989/sss.2020.26.5.575

Cable vibration control with internal and external dampers: Theoretical analysis and field test validation

Fangdian Di[1a], Limin Sun[1,2b] and Lin Chen[*1]

[1]*Department of Bridge Engineering, Tongji University, 1239 Siping Road, Shanghai, China*
[2]*State key Laboratory for Disaster Reduction in Civil Engineering, Tongji University, 1239 Siping Road, Shanghai, China*

(*Received October 19, 2019, Revised July 13, 2020, Accepted August 22, 2020*)

Abstract. For vibration control of stay cables in cable-stayed bridges, viscous dampers are frequently used, and they are regularly installed between the cable and the bridge deck. In practice, neoprene rubber bushings (or of other types) are also widely installed inside the cable guide pipe, mainly for reducing the bending stresses of the cable near its anchorages. Therefore, it is important to understand the effect of the bushings on the performance of the external damper. Besides, for long cables, external dampers installed at a single position near a cable end can no longer provide enough damping due to the sag effect and the limited installation distance. It is thus of interest to improve cable damping by additionally installing dampers inside the guide pipe. This paper hence studies the combined effects of an external damper and an internal damper (which can also model the bushings) on a stay cable. The internal damper is assumed to be a High Damping Rubber (HDR) damper, and the external damper is considered to be a viscous damper with intrinsic stiffness, and the cable sag is also considered. Both the cases when the two dampers are installed close to one cable end and respectively close to the two cable ends are studied. Asymptotic design formulas are derived for both cases considering that the dampers are close to the cable ends. It is shown that when the two dampers are placed close to different cable ends, their combined damping effects are approximately the sum of their separate contributions, regardless of small cable sag and damper intrinsic stiffness. When the two dampers are installed close to the same end, maximum damping that can be achieved by the external damper is generally degraded, regardless of properties of the HDR damper. Field tests on an existing cable-stayed bridge have further validated the influence of the internal damper on the performance of the external damper. The results suggest that the HDR is optimally placed in the guide pipe of the cable-pylon anchorage when installing viscous dampers at one position is insufficient. When an HDR damper or the bushing has to be installed near the external damper, their combined damping effects need to be evaluated using the presented methods.

Keywords: stay cable; vibration control; sag effect; viscous damper; HDR damper; modal damping; parameter optimization

1. Introduction

Cables are widely used in structural engineering because of their high axial strength-to-weight ratio (Irvine 1981). However, due to their high flexibility in the lateral direction and low intrinsic damping, they are prone to vibrations induced by various types of excitations (De Sá Caetano 2007, Fujino *et al*. 2012, Hikami and Shiraishi 1988, Matsumoto *et al*. 2001). Mechanical dampers are commonly installed on long cables to increase cable energy dissipation capacity and thus suppress cable vibrations (Chen *et al*. 2003).

The research on the cable-damper system can be traced back to the 1980s. Carne (1981) and Kovacs (1982) were among the first researchers to investigate the vibrations of a taut cable with an attached damper, both focusing on the first-mode damping ratio when the damper location is near one cable end. Later, Yoneda and Maeda (1989), Uno *et al*. (1991) and Pacheco *et al*. (1993) attempted to develop universal design formulas for a taut cable with a viscous damper by using the complex eigenanalysis method. By grouping the non-dimensional damper/cable parameters properly, Pacheco *et al*. (1993) managed to obtain the "universal estimation curve" which applies to the first several cable modes for a damper at an arbitrary location close to a cable end. Xu and Yu (1998a, b) developed an efficient and accurate transfer matrix formulation using complex eigenfunctions and focused on the influences of sag and out-plane vibrations. Krenk (2000) developed an exact analytical formulation of the frequency equation of a taut cable with a viscous damper and obtained an asymptotic approximation for the damping ratios of the first few modes for damper locations near one cable end. Subsequently, the analytical method has been extended to consider cable sag (Krenk and Nielson 2002). Main and Jones (2002a, b) followed the same approach and analyzed the case of a damper located arbitrarily along the cable. They pointed out the importance of damper-induced frequency shifts in characterizing the response of the system. Furthermore, to simulate realistic cable-damper systems, more cable parameters have been included, such as

*Corresponding author, Research Associate Professor, E-mail: linchen@tongji.edu.cn
[a] Ph.D. Student, E-mail: fangdiandi@tongji.edu.cn
[b] Professor, E-mail: lmsun@tongji.edu.cn

ISSN: 1738-1584 (Print), 1738-1991 (Online)

the bending stiffness (Main and Jones 2007, Fujino and Hoang 2008), cable sag (Xu and Yu 1998a, b, Yu and Xu 1998, Wang *et al*. 2005, Nielsen and Krenk 2003, Krenk and Nielsen 2002, Fujino and Hoang 2008) and inclination (Xu and Yu 1998a, Fujino and Hoang 2008, Hoang and Fujino 2007, Sun and Huang 2008). Besides, dampers beside an ideally viscous type have been addressed, such as taking into account the damper intrinsic stiffness (Zhou and Sun 2006), nonlinearity (Main and Jones 2002a, b, Chen and Sun 2016, Sun *et al*. 2019b) and damper support flexibility (Fujino and Hoang 2008, Sun and Huang 2008) and damper mass (Duan *et al*. 2019a, b).

However, as cables are increasingly long in long-span cable-stayed bridges, a single damper installation may no longer be able to provide enough damping. Caracoglia and Jones (2007) hence investigated the combined damping effect of two viscous dampers on a stay cable. Their result suggests that the use of dampers in close position cannot enhance the maximum attainable modal damping in the cable. In contrast, dampers at opposite ends can increase the supplemental damping. A similar conclusion has been arrived by Hoang and Fujino (2008). Zhou *et al*. (2014) had studied a taut cable with a damper and a spring while the position of the spring was arbitrary along the cable. Cu *et al*. (2015) investigated the damping of a cable equipped with two HDR dampers. Other methods for enhancing near-anchorage damper performance have also been explored recently, for example, by using a passive negative stiffness device (Chen *et al*. 2015, Zhou and Li 2016). Particularly, a viscous damper combined with pre-compressed springs was studied by Chen *et al*. (2015). Chen *et al*. (2016) has proposed to use both rotational and transverse dampers for supplementing cable damping. Inerter devices have also been combined with viscous dampers for cable vibration control (Sun *et al*. 2017, Lu *et al*. 2017, 2019, Wang *et al*. 2019, Huang *et al*. 2019).

It is noted that in practice, rubber bushings (or other types) are commonly installed inside steel guide pipes at cable anchorages for reducing cable bending stress near the ends (Nakamura *et al*. 1998). The bushings have been modeled as springs in the previous studies, while they also have some energy dissipation effects. Takano *et al*. (1997) found that the stiffness of the bushing could significantly reduce damper effectiveness. Main and Jones (2003) analyzed a taut cable with a bushing (linear spring) and a viscous damper (linear dashpot), and an asymptotic solution is obtained which leads a generalized design curve for a linear viscous damper accounting for the bushing stiffness.

When a single external damper is inadequate for cable vibration control, it is straightforward to replace the bushing by an HDR damper, referred to as the internal damper in the guide pipe. Practically, this is more feasible than other strategies such as installing dampers near both cable ends. Indeed, the combination of a viscous damper and an HDR damper mounted at opposite ends was studied by Hoang and Fujino (2008), and it was found that the total damping is approximately the sum of their separate damping effect. However, the case of a viscous damper and an HDR damper installed at the same end has not been studied till date. Besides, in the previous studies concerning two dampers on a cable, cable sag and damper intrinsic stiffness have not been investigated in detail. Notably, Yoneda *et al*. (1995) studied two dampers with stiffness near the same cable end but using an approximate method based on the equivalence of the damper parameters or the installation position. Therefore, this study performs a comprehensive analysis of the damping effect of a shallow cable attached with an external damper and an internal damper. The external damper is considered to be a viscous damper with intrinsic stiffness, and the internal one is described using an HDR model, which can simulate both the bushings and also the rubber dampers. Asymptotic formulas for modal damping ratios are derived when both the external and internal dampers are close to cable anchorages, either on the same end or opposite ends of a cable. Parametric analysis is then carried out to discuss their joint effects, particularly, on multimode cable damping. For the case when the two dampers are installed close to the same cable end, an experimental study has been conducted to validate the theoretical estimation.

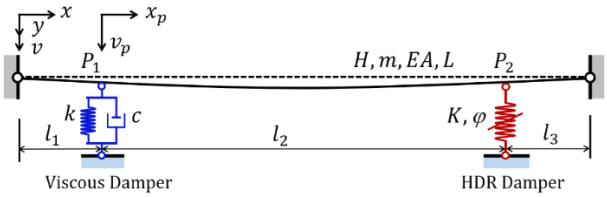

Fig. 1 A shallow cable with an internal damper and an external damper

The rest of this paper is organized as follows. Sec. 2 presents the characteristic equation of the system using the complex modal analysis. Sec. 3 derives asymptotic solutions for cases when the dampers are installed respectively close to the two cable ends and close to the same cable end, and performs the parametric analysis. Sec. 4 introduces the experimental study and compares the results. Sec. 5 concludes the paper.

2. Characteristic equations of a shallow cable with both internal and external dampers

A shallow cable with an internal damper and an external damper is shown in Fig. 1. The cable is fixed at both ends. The cable chord length is denoted by L, the cable axial tension is indicated by H, the mass per unit length is denoted by m, and the axial stiffness is denoted by EA. The external damper is a viscous damper with intrinsic stiffness, and k and c are the stiffness and damping coefficients respectively; and, it is installed close to one cable end at a distance of l_1. The internal damper is an HDR damper with stiffness K and loss factor φ, and the distance of the HDR from the nearer cable end is denoted by l_3. As long cables are concerned here, cable bending stiffness is neglected. Cable inherent damping is ignored as it is practically very small.

For describing static profile and dynamic displacements of the cable, a coordinate system is defined for the cable-

damper system with x starting from the left cable anchorage pointing rightwards along the cable chord, and the static profile and the dynamic displacement are denoted by $y(x)$ and $v(x,t)$, respectively, with t = time.

The static profile of a shallow cable can be accurately approximated by the parabolic function (Irvine 1981)

$$y(x) = 4f\left(1-\frac{x}{L}\right)\frac{x}{L}, \qquad f = \frac{mgL^2}{8H} \tag{1}$$

The sag at cable mid-span is denoted by f, and g is the gravitational acceleration. Cable inclination can be considered in the definition of the non-dimensional sag parameter (Irvine 1981).

The cable is divided by the two dampers into three cable elements, and the connection points are denoted by P_p with index $p = 0, 1, 2, 3$. Where P_0 and P_3 correspond to the left and right anchorages of the cable, and P_1 and P_2 correspond to the left and right damper installation points respectively. An element-wise coordinate system is defined with the horizontal axis x_p starting from P_{p-1} pointing towards P_p, as shown in Fig. 1. A typical element p is a segment with a length of l_p between the points P_{p-1} and P_p, and its vertical dynamic displacement is denoted by $v_p(x_p,t)$. The cable vibration induces an additional horizontal tension $h(t)$. Thus, the equation of each cable segment is governed by the following partial differential equation (Irvine and Caughey 1974) as

$$H\frac{\partial^2 v_p}{\partial {x_p}^2} + h\frac{\mathrm{d}^2 y}{\mathrm{d}x^2} = m\frac{\partial^2 v_p}{\partial t^2} \tag{2}$$

The dynamic cable tension h can be obtained from the elastic elongation of the cable. Denote the initial length of the cable element as $\mathrm{d}s$ and the element length after elastic elongation as $\mathrm{d}s'$. The increment of the cable tension along the chord is $h(\mathrm{d}s/\mathrm{d}x)$, and thus the elasticity relation of the cable can be written as

$$\frac{h}{EA}\frac{\mathrm{d}s}{\mathrm{d}x} = \frac{\mathrm{d}s'-\mathrm{d}s}{\mathrm{d}s} \cong \frac{\mathrm{d}x}{\mathrm{d}s}\frac{\mathrm{d}u}{\mathrm{d}s} + \frac{\mathrm{d}y}{\mathrm{d}s}\frac{\mathrm{d}v}{\mathrm{d}s} \tag{3}$$

where $u(x,t)$ denotes the cable dynamic displacement along the chord and the last relation follows from the motion of a point from its initial position (x,y) to $(x+u, y+v)$. Including the boundary conditions of $u(x,t)$ and $v(x,t)$ at the cable anchorages, multiplying Eq. (3) by $(\mathrm{d}s/\mathrm{d}x)^2$ and then integrating the left- and right-hand sides over the cable span, one obtains

$$\frac{hL_e}{EA} = \frac{mg}{H}\int_0^L v(x,t)\,\mathrm{d}x = \frac{mg}{H}\sum_{p=1}^{3}\int_0^{l_p} v_p(x_p,t)\,\mathrm{d}x_p \tag{4}$$

where

$$L_e = \int_0^L (\mathrm{d}s/\mathrm{d}x)^3\mathrm{d}x \cong [1+8(f/L)^2]L$$

Considering free in-plane vibrations of the cable, solutions to Eq. (2) are expressed as

$$v_p(x_p,t) = \tilde{v}_p\exp(\mathrm{i}\omega t), \qquad h(t) = \tilde{h}\exp(\mathrm{i}\omega t) \tag{5}$$

where ω is the complex circular frequency, $\mathrm{i} = \sqrt{-1}$, $\tilde{v}_p$ and $\tilde{h}$ denote the complex vibration amplitudes of the corresponding time-dependent variables. Substituting Eq. (5) into Eq. (2), one finds

$$\frac{\mathrm{d}^2\tilde{v}_p}{\mathrm{d}x_p^2} + \beta^2\tilde{v}_p = \frac{8f}{L^2}\frac{\tilde{h}}{H} \tag{6}$$

where $\beta = \omega\sqrt{m/H}$ is the wavenumber.

Similarly, Eq. (4) becomes

$$\frac{\tilde{h}L_e}{EA} = \frac{mg}{H}\sum_{p=1}^{3}\int_0^{l_p}\tilde{v}_p(x_p)\,\mathrm{d}x_p \tag{7}$$

The transverse vibrations of a general cable element at its left and right ends are denoted by $v_{p-1}(t)$ and $v_p(t)$ respectively. In free vibrations of the cable, one finds $v_{p-1}(t) = \tilde{v}_{p-1}\exp(\mathrm{i}\omega t)$ and $v_p(t) = \tilde{v}_p\exp(\mathrm{i}\omega t)$. The solutions of $\tilde{v}_p$ can then be obtained, as

$$\begin{aligned}&\tilde{v}_p(x_p) = \tilde{v}_{p-1}[\cos(\beta x_p) - \cot(\beta l_p)\sin(\beta x_p)] + \tilde{v}_p\\ &\frac{\sin(\beta x_p)}{\sin(\beta l_p)} + \frac{8f}{(\beta L)^2}\frac{\tilde{h}}{H}\left[1-\cos(\beta x_p) - \tan\frac{\beta l_p}{2}\sin(\beta x_p)\right]\end{aligned} \tag{8}$$

Noting that

$$\begin{aligned}&\int_0^{l_p}\tilde{v}_p(x_p)\,\mathrm{d}x_p\\ &= \frac{8f}{(\beta L)^2}\frac{\tilde{h}}{H}l_p + \frac{1}{\beta}\tan\frac{\beta l_p}{2}\left[\tilde{v}_{p-1} + \tilde{v}_p - \frac{16f}{(\beta L)^2}\frac{\tilde{h}}{H}\right]\end{aligned} \tag{9}$$

Eq. (7) becomes

$$\begin{aligned}&\frac{8f\tilde{h}}{H}\left[\frac{1}{(\beta L)^2} - \frac{1}{\lambda^2}\right]\\ &+\sum_{p=1}^{3}\left\{\frac{1}{\beta L}\tan\frac{\beta l_p}{2}\left[\tilde{v}_{p-1} + \tilde{v}_p - \frac{16f}{(\beta L)^2}\frac{\tilde{h}}{H}\right]\right\} = 0\end{aligned} \tag{10}$$

where the Irvine parameter is defined as

$$\lambda^2 = \left(\frac{mgL}{H}\right)^2 L\frac{EA}{HL_e}$$

Eq. (10) is multiplied by $(\beta L)^3$, leading to

$$\begin{aligned}&\frac{8f\tilde{h}}{H}\left[\beta L - \frac{(\beta L)^3}{\lambda^2}\right]\\ &+\sum_{p=1}^{3}\left\{(\beta L)^2\tan\frac{\beta l_p}{2}\left[\tilde{v}_{p-1} + \tilde{v}_p - \frac{16f}{(\beta L)^2}\frac{\tilde{h}}{H}\right]\right\} = 0\end{aligned} \tag{11}$$

From Eq. (8), one finds the following expressions

$$\left.\frac{\mathrm{d}\tilde{v}_p}{\mathrm{d}x_p}\right|_{x_p=0} = -\tilde{v}_{p-1}\beta\cot(\beta l_p) + \tilde{v}_p\beta\frac{1}{\sin(\beta l_p)} - \frac{8f}{(\beta L)^2}\frac{\tilde{h}}{H}\beta\tan\frac{\beta l_p}{2} \tag{12a}$$

$$\left.\frac{\mathrm{d}\tilde{v}_p}{\mathrm{d}x_p}\right|_{x_p=l_p} = -\tilde{v}_{p-1}\beta\frac{1}{\sin(\beta l_p)} + \tilde{v}_p\beta\cot(\beta l_p) + \frac{8f}{(\beta L)^2}\frac{\tilde{h}}{H}\beta\tan\frac{\beta l_p}{2} \tag{12b}$$

The internal force equilibrium at the damper location is expressed as

$$H\left(\left.\frac{\mathrm{d}\tilde{v}_{p+1}}{\mathrm{d}x_{p+1}}\right|_{x_{p+1}=0} - \left.\frac{\mathrm{d}\tilde{v}_p}{\mathrm{d}x_p}\right|_{x_p=l_p}\right) = \frac{\tilde{v}_{p-1}H\beta}{\sin(\beta l_p)} - \tilde{v}_pH\beta\left[\cot(\beta l_p)+\cot(\beta l_{p+1})\right] + \frac{\tilde{v}_{p+1}H\beta}{\sin(\beta l_{p+1})} - \frac{8f}{(\beta L)^2}\frac{\tilde{h}}{H}H\beta\left(\tan\frac{\beta l_p}{2}+\tan\frac{\beta l_{p+1}}{2}\right) = f_i, \qquad i=1,2 \tag{13}$$

where $f_1 = (k+\mathrm{i}\omega c)\tilde{v}_1$ is the force-deformation relation of the external damper expressed in the frequency domain, and $f_2 = K(1+\mathrm{i}\varphi)\tilde{v}_2$ represents the force-deformation relation of the HDR damper in the frequency domain (Fujino and Hoang 2008). Note that subscripts 1 and 2 correspond to the viscous damper and HDR damper, respectively.

Finally, collecting Eqs. (11) and (13) and after simplification, three equations are obtained as

$$\frac{8f\tilde{h}}{H}\left[\beta L - \frac{(\beta L)^3}{\lambda^2} - 2\left(\tan\frac{\beta l_1}{2}+\tan\frac{\beta l_2}{2}+\tan\frac{\beta l_3}{2}\right)\right] + (\beta L)^2\tilde{v}_1\left(\tan\tfrac{\beta l_1}{2}+\tan\tfrac{\beta l_2}{2}\right) + (\beta L)^2\tilde{v}_2\left(\tan\tfrac{\beta l_2}{2}+\tan\tfrac{\beta l_3}{2}\right) = 0 \tag{14a}$$

$$-\tilde{v}_1[\cot(\beta l_1)+\cot(\beta l_2)] + \frac{\tilde{v}_2}{\sin(\beta l_2)} - \frac{8f}{(\beta L)^2}\frac{\tilde{h}}{H}\left(\tan\frac{\beta l_1}{2}+\tan\frac{\beta l_2}{2}\right) = \frac{k+\mathrm{i}\omega c}{H\beta}\tilde{v}_1 \tag{14b}$$

$$\frac{\tilde{v}_1}{\sin(\beta l_2)} - \tilde{v}_2[\cot(\beta l_2)+\cot(\beta l_3)] - \frac{8f}{(\beta L)^2}\frac{\tilde{h}}{H}\left(\tan\frac{\beta l_2}{2}+\tan\frac{\beta l_3}{2}\right) = \frac{K(1+\mathrm{i}\varphi)}{H\beta}\tilde{v}_2 \tag{14c}$$

Eq. (14) can be written in a matrix form as

$$\begin{bmatrix} (\beta L)^2B_1 & (\beta L)^2B_2 & \Omega \\ -D_1-\xi_1 & C & -B_1(\beta L)^{-2} \\ C & -D_2-\xi_2 & -B_2(\beta L)^{-2} \end{bmatrix}\begin{bmatrix}\tilde{v}_1\\ \tilde{v}_2\\ 8f\tilde{h}H^{-1}\end{bmatrix} = 0 \tag{15}$$

where 0 is a zero vector and

$$B_1 = \tan\frac{\beta l_1}{2}+\tan\frac{\beta l_2}{2}, \quad B_2 = \tan\frac{\beta l_2}{2}+\tan\frac{\beta l_3}{2}$$
$$C = \frac{1}{\sin(\beta l_2)}, \qquad D_1 = \cot(\beta l_1)+\cot(\beta l_2)$$
$$D_2 = \cot(\beta l_2)+\cot(\beta l_3)$$
$$\Omega = 2\left[\frac{\beta L}{2} - \frac{4}{\lambda^2}\left(\frac{\beta L}{2}\right)^3 - \sum_{p=1}^{3}\tan\frac{\beta l_p}{2}\right]$$
$$\xi_1 = \frac{k+\mathrm{i}\omega c}{\omega\sqrt{mH}}, \qquad \xi_2 = \frac{K(1+\mathrm{i}\varphi)}{\omega\sqrt{mH}}$$

The characteristic equation of the system is given by the determinant of the coefficient matrix in Eq. (15). After simplification, the following equation is obtained

$$\Theta + 2\Xi_1\xi_1 + 2\Xi_2\xi_2 + 4\Lambda\xi_1\xi_2 = 0 \tag{16}$$

where

$$\Theta = \sin\frac{\beta L}{2}\left\{\sin\frac{\beta L}{2} - \left[\frac{\beta L}{2} - \frac{4}{\lambda^2}\left(\frac{\beta L}{2}\right)^3\right]\cos\frac{\beta L}{2}\right\}$$
$$\Xi_1 = \sin\frac{\beta(L-l_1)}{2}\sin\frac{\beta l_1}{2}\times \left\{\sin\frac{\beta L}{2} - \cos\frac{\beta l_1}{2}\cos\frac{\beta(L-l_1)}{2}\left[\frac{\beta L}{2} - \frac{4}{\lambda^2}\left(\frac{\beta L}{2}\right)^3\right]\right\}$$
$$\Xi_2 = \sin\frac{\beta(L-l_3)}{2}\sin\frac{\beta l_3}{2}\times \left\{\sin\frac{\beta L}{2} - \cos\frac{\beta l_3}{2}\cos\frac{\beta(L-l_3)}{2}\left[\frac{\beta L}{2} - \frac{4}{\lambda^2}\left(\frac{\beta L}{2}\right)^3\right]\right\}$$
$$\Lambda = \prod_{p=1}^{3}\sin\frac{\beta l_p}{2}\times \left\{\sin\frac{\beta L}{2} + \prod_{p=1}^{3}\sin(\beta l_p) - \left[\frac{\beta L}{2} - \frac{4}{\lambda^2}\left(\frac{\beta L}{2}\right)^3\right]\prod_{p=1}^{3}\cos\frac{\beta l_p}{2}\right\}$$

For limiting cases related to particular values of ξ_1 and ξ_2, the solutions to Eq. (16) are discussed as follows.

1) When $\xi_1 = \xi_2 = 0$, Eq. (16) simply becomes $\Theta = 0$, whose solutions correspond to the eigenfrequencies of a shallow cable without any attachments.

2) When $\xi_1 = 0$ or $\xi_2 = 0$, only one damper is attached to the cable. For example, let $\xi_1 = \xi$ and $\xi_2 = 0$, Eq. (16) reduces to $\Theta + 2\Xi_1\xi = 0$, corresponding to the characteristic equation of a shallow cable with a viscous damper, as discussed by Krenk and Nielsen (2002) where the damper stiffness was absent though.

3) When $\xi_1 = \xi_2 \to \propto$, Eq. (16) is reduced to $\Lambda = 0$, which gives solutions to the "locked-damper" modes of the cable, i.e., no vertical displacement at the two nodes, P_1 and P_2. Two groups of solutions are obtained when the factors in the left-hand side of $\Lambda = 0$ are respectively equal to zero. These are real oscillatory modes characterized by the three segments of the cable oscillating independently (Sun *et al.* 2019a).

4) Other limiting cases include that either ξ_1 or ξ_2 is infinite, leading to a system similar to a single shallow cable with a damper (Krenk and Nielsen 2002, Fujino and Hoang 2008), which is hence not discussed any more.

3. Modal damping of a cable with both internal and external dampers

Providing cable parameters, damper properties and

damper locations, the wavenumber can be solved from Eq. (16) numerically for modes of concern. Here, the argument principle method (Chen *et al.* 2016) is used when necessary. For normal cases when dampers are close to a cable end, asymptotic formulas of the complex wavenumber are derived for lower modes. The derivation is based on a small perturbation on the real wavenumber of a cable without any attachments. Recall that the wavenumber of a shallow cable, denoted by β_n^0 with superscript 0 indicating no damper attached and n the mode index, is given by

$$\tan\frac{\beta_n^0 L}{2} = \frac{\beta_n^0 L}{2} - \frac{4}{\lambda^2}\left(\frac{\beta_n^0 L}{2}\right)^3, \qquad n = 1,3,\cdots \tag{17}$$

$$\beta_n^0 = \frac{n\pi}{L}, \qquad n = 2,4,\cdots \tag{18}$$

The complex wavenumber β_n can be assumed a small perturbation from β_n^0 as $\Delta\beta_n = \beta_n - \beta_n^0$. Once the wavenumber is obtained, the modal damping is determined afterwards by

$$\zeta_n = \frac{\mathrm{Im}[\omega_n]}{|\omega_n|} = \frac{\mathrm{Im}[\beta_n]}{|\beta_n|} \cong \frac{\mathrm{Im}[\Delta\beta_n]}{\beta_n^0} \tag{19}$$

3.1 Dampers at the opposite ends

3.1.1 Nearly antisymmetric mods

Eq. (16) can be written as

$$\begin{aligned}
\tan\frac{\beta L}{2} = \frac{\begin{aligned}
&2\sin^2\left(\frac{\beta l_1}{2}\right)\left\{\sin\frac{\beta L}{2} - \cos\frac{\beta l_1}{2}\cos\frac{\beta(L-l_1)}{2}\left[\frac{\beta L}{2} - \frac{4}{\lambda^2}\left(\frac{\beta L}{2}\right)^3\right]\right\}\xi_1 \\
&+ 2\sin^2\left(\frac{\beta l_3}{2}\right)\left\{\sin\frac{\beta L}{2} - \cos\frac{\beta l_3}{2}\cos\frac{\beta(L-l_3)}{2}\left[\frac{\beta L}{2} - \frac{4}{\lambda^2}\left(\frac{\beta L}{2}\right)^3\right]\right\}\xi_2 \\
&+ 4\sin\frac{\beta(l_1+l_3)}{2}\sin\frac{\beta l_1}{2}\sin\frac{\beta l_3}{2}\left\{\sin\frac{\beta L}{2} + \prod_{p=1}^{3}\sin(\beta l_p) - \left[\frac{\beta L}{2} - \frac{4}{\lambda^2}\left(\frac{\beta L}{2}\right)^3\right]\prod_{p=1}^{3}\cos\frac{\beta l_p}{2}\right\}\xi_1\xi_2
\end{aligned}}{\begin{aligned}
&\left\{\sin\frac{\beta L}{2} - \left[\frac{\beta L}{2} - \frac{4}{\lambda^2}\left(\frac{\beta L}{2}\right)^3\right]\cos\frac{\beta L}{2}\right\} \\
&+ \sin(\beta l_1)\left\{\sin\frac{\beta L}{2} - \cos\frac{\beta l_1}{2}\cos\frac{\beta(L-l_1)}{2}\left[\frac{\beta L}{2} - \frac{4}{\lambda^2}\left(\frac{\beta L}{2}\right)^3\right]\right\}\xi_1 \\
&+ \sin(\beta l_3)\left\{\sin\frac{\beta L}{2} - \cos\frac{\beta l_3}{2}\cos\frac{\beta(L-l_3)}{2}\left[\frac{\beta L}{2} - \frac{4}{\lambda^2}\left(\frac{\beta L}{2}\right)^3\right]\right\}\xi_2 \\
&+ 4\cos\frac{\beta(l_1+l_3)}{2}\sin\frac{\beta l_1}{2}\sin\frac{\beta l_3}{2}\left\{\sin\frac{\beta L}{2} + \prod_{p=1}^{3}\sin(\beta l_p) - \left[\frac{\beta L}{2} - \frac{4}{\lambda^2}\left(\frac{\beta L}{2}\right)^3\right]\prod_{p=1}^{3}\cos\frac{\beta l_p}{2}\right\}\xi_1\xi_2
\end{aligned}}
\end{aligned} \tag{20}$$

The asymptotic result is obtained from Eq. (20) by assuming $\beta_n \cong \beta_n^0$ in the right-hand side. The wavenumber equation then reduces to

$$\tan\frac{\beta L}{2} \cong \frac{\frac{1}{2}\sin^2(\beta l_1)\xi_1 + \frac{1}{2}\sin^2(\beta l_3)\xi_2 - \frac{1}{2}\sin(\beta l_1)\sin(\beta l_2)\sin(\beta l_3)\xi_1\xi_2}{1 + \sin(\beta l_1)\cos^2\left(\frac{\beta l_1}{2}\right)\xi_1 + \sin(\beta l_3)\cos^2\left(\frac{\beta l_3}{2}\right)\xi_2 + \cos^2\left(\frac{\beta l_2}{2}\right)\sin(\beta l_1)\sin(\beta l_3)\xi_1\xi_2} \tag{21}$$

The asymptotic expression valid for $l_1 \ll L$ and $l_3 \ll L$ is further obtained by introducing the approximation that $\tan\frac{\beta L}{2} \cong 0.5\Delta\beta_n L$, and using the one-term Taylor expansion of the sine and cosine terms on the right-hand side. The wavenumber increment is then explicitly expressed as

$$\Delta\beta_n \cong \frac{\beta_n^0}{L}\frac{\beta_n^0(l_1)^2\xi_1 + \beta_n^0(l_3)^2\xi_2 + l_1\beta_n^0(l_1+l_3)\beta_n^0 l_3\xi_1\xi_2}{1+\beta_n^0 l_1\xi_1 + \beta_n^0 l_3\xi_2 + \beta_n^0 l_1\beta_n^0 l_3\xi_1\xi_2} \tag{22}$$

It is convenient to introduce the non-dimensional damper parameters as

$$\bar{c} = \frac{c}{\sqrt{Hm}}, \quad \bar{k} = \frac{kl_1}{H}, \quad \bar{K} = \frac{Kl_3}{H},$$

where $\bar{c}$ is the dimensionless viscous coefficient, $\bar{k}$ is the dimensionless damper stiffness, and $\bar{K}$ is the dimensionless spring coefficient of the HDR damper. Furthermore, define the following group parameter $\kappa = \bar{c}l_1\beta_n^0$. Eq. (22) thus becomes

$$\begin{aligned}
&\Delta\beta_n \cong \frac{\beta_n^0}{L}\times \\
&\frac{l_1(\bar{k}+\mathrm{i}\kappa) + l_3(\bar{K}+\mathrm{i}\varphi\bar{K}) + (l_1+l_3)(\bar{k}+\mathrm{i}\kappa)(\bar{K}+\mathrm{i}\varphi\bar{K})}{1+(\bar{k}+\mathrm{i}\kappa) + (\bar{K}+\mathrm{i}\varphi\bar{K}) + (\bar{k}+\mathrm{i}\kappa)(\bar{K}+\mathrm{i}\varphi\bar{K})}
\end{aligned} \tag{23}$$

The damping ratio can then be extracted from the complex wavenumber using Eq. (19), leading to

$$\begin{aligned}
&\zeta_n \cong \frac{1}{L}\\
&\frac{\begin{aligned}&[l_1\kappa + l_3\varphi\bar{K} + (l_1+l_3)(\bar{k}\varphi\bar{K}+\kappa\bar{K})](1+\bar{k}+\bar{K}+\bar{k}\bar{K}-\kappa\varphi\bar{K}) \\ &-[l_1\bar{k} + l_3\bar{K} + (l_1+l_3)(\bar{k}\bar{K}-\kappa\varphi\bar{K})](\kappa+\varphi\bar{K}+\bar{k}\varphi\bar{K}+\kappa\bar{K})\end{aligned}}{(1+\bar{k}+\bar{K}+\bar{k}\bar{K}-\kappa\varphi\bar{K})^2 + (\kappa+\varphi\bar{K}+\bar{k}\varphi\bar{K}+\kappa\bar{K})^2} \\
&n = 2,4,\cdots
\end{aligned} \tag{24}$$

Further simplification of Eq. (24) gives

$$\zeta_n \cong \frac{\kappa}{(1+\bar{k})^2+\kappa^2}\frac{l_1}{L} + \frac{\varphi\bar{K}}{(1+\bar{K})^2+\varphi^2\bar{K}^2}\frac{l_3}{L}, \quad n = 2,4,\cdots \tag{25}$$

Eq. (25) is the asymptotic modal damping of the cable with an internal damper and an external damper when they are respectively close to the two cable ends. The expression includes two terms, corresponding to the contribution of each of the two dampers. The maximum modal damping ratio in the cable is achieved when each damper is respectively under the optimal condition, that is

$$\kappa_{\mathrm{opt}} \cong 1+\bar{k}, \qquad \bar{K}_{\mathrm{opt}} = \frac{1}{\sqrt{1+\varphi^2}}$$

$$\zeta_{n,\mathrm{opt}} \cong 0.5\frac{1}{1+\bar{k}}\frac{l_1}{L}+0.5\frac{\varphi}{1+\sqrt{1+\varphi^2}}\frac{l_3}{L}$$

When the loss factor φ is zero, the HDR damper is reduced to a spring with stiffness $\bar{K}$, and the second term of Eq. (25) equals zero. When the spring factor of the HDR damper is infinite, the second term of Eq. (25) also equals zero. In those special cases, the HDR damper has no contribution to the cable modal damping.

3.1.2 Nearly symmetric modes

Eq. (16) can be rewritten as

$$\begin{aligned}
&\sin\frac{\beta L}{2}\left\{\sin\frac{\beta L}{2}-\left[\frac{\beta L}{2}-\frac{4}{\lambda^2}\left(\frac{\beta L}{2}\right)^3\right]\cos\frac{\beta L}{2}\right\}=-2\sin\frac{\beta(L-l_1)}{2}\\
&\sin\frac{\beta l_1}{2}\left\{\sin\frac{\beta L}{2}-\cos\frac{\beta l_1}{2}\cos\frac{\beta(L-l_1)}{2}\left[\frac{\beta L}{2}-\frac{4}{\lambda^2}\left(\frac{\beta L}{2}\right)^3\right]\right\}\xi_1\\
&-2\sin\frac{\beta(L-l_3)}{2}\sin\frac{\beta l_3}{2}\left\{\sin\frac{\beta L}{2}-\cos\frac{\beta l_3}{2}\cos\frac{\beta(L-l_3)}{2}\right.\\
&\left.\left[\frac{\beta L}{2}-\frac{4}{\lambda^2}\left(\frac{\beta L}{2}\right)^3\right]\right\}\xi_2-4\prod_{p=1}^{3}\sin\frac{\beta l_p}{2}\left\{\sin\frac{\beta L}{2}+\right.\\
&\left.\prod_{p=1}^{3}\sin(\beta l_p)-\left[\frac{\beta L}{2}-\frac{4}{\lambda^2}\left(\frac{\beta L}{2}\right)^3\right]\prod_{p=1}^{3}\cos\frac{\beta l_p}{2}\right\}\xi_1\xi_2
\end{aligned}\tag{26}$$

The left- and right-hand sides of Eq. (26) are divided by $\sin\frac{\beta L}{2}\cos\frac{\beta L}{2}$, leading to

$$\begin{aligned}
&\left\{\tan\frac{\beta L}{2}-\left[\frac{\beta L}{2}-\frac{4}{\lambda^2}\left(\frac{\beta L}{2}\right)^3\right]\right\}\\
&\left\{\begin{array}{c}1+2\sin\frac{\beta(L-l_1)}{2}\sin\frac{\beta l_1}{2}\sin^{-1}\left(\frac{\beta L}{2}\right)\xi_1+2\sin\frac{\beta(L-l_3)}{2}\sin\frac{\beta l_3}{2}\sin^{-1}\left(\frac{\beta L}{2}\right)\xi_2\\ +4\sin^{-1}\left(\frac{\beta L}{2}\right)\prod_{p=1}^{3}\sin\frac{\beta l_p}{2}\left\{1+\sin^{-1}\left(\frac{\beta L}{2}\right)\prod_{p=1}^{3}\sin(\beta l_p)-\left[\frac{\beta L}{2}-\frac{4}{\lambda^2}\left(\frac{\beta L}{2}\right)^3\right]\sin^{-1}\left(\frac{\beta L}{2}\right)\prod_{p=1}^{3}\cos\frac{\beta l_p}{2}\right\}\xi_1\xi_2\end{array}\right\}=\sin^{-1}\left(\frac{\beta L}{2}\right)\\
&\left[\frac{\beta L}{2}-\frac{4}{\lambda^2}\left(\frac{\beta L}{2}\right)^3\right]\left\{-2\sin\frac{\beta(L-l_1)}{2}\sin\frac{\beta l_1}{2}\left[1-\cos^{-1}\left(\frac{\beta L}{2}\right)\cos\frac{\beta(L-l_1)}{2}\cos\frac{\beta l_1}{2}\right]\xi_1-2\sin\frac{\beta(L-l_3)}{2}\sin\frac{\beta l_3}{2}\left[1-\cos^{-1}\left(\frac{\beta L}{2}\right)\right.\right.\\
&\left.\left.\cos\frac{\beta(L-l_3)}{2}\cos\frac{\beta l_3}{2}\right]\xi_2-4\prod_{p=1}^{3}\sin\frac{\beta l_p}{2}\left\{1+\sin^{-1}\left(\frac{\beta L}{2}\right)\prod_{p=1}^{3}\sin(\beta l_p)-\left[\frac{\beta L}{2}-\frac{4}{\lambda^2}\left(\frac{\beta L}{2}\right)^3\right]\sin^{-1}\left(\frac{\beta L}{2}\right)\prod_{p=1}^{3}\cos\frac{\beta l_p}{2}\right\}\xi_1\xi_2\right\}
\end{aligned}\tag{27}$$

Noting that

$$\begin{gathered}
\frac{\cos\frac{\beta l_1}{2}\cos\frac{\beta(L-l_1)}{2}}{\cos\frac{\beta L}{2}}=1+\frac{\sin\frac{\beta l_1}{2}\sin\frac{\beta(L-l_1)}{2}}{\cos\frac{\beta L}{2}},\quad \frac{\cos\frac{\beta l_3}{2}\cos\frac{\beta(L-l_3)}{2}}{\cos\frac{\beta L}{2}}=1+\frac{\sin\frac{\beta l_3}{2}\sin\frac{\beta(L-l_3)}{2}}{\cos\frac{\beta L}{2}}\\
\frac{\cos\frac{\beta l_1}{2}\cos\frac{\beta l_2}{2}\cos\frac{\beta l_3}{2}}{\cos\frac{\beta L}{2}}\cong 1+\frac{\sin\frac{\beta(l_1+l_3)}{2}\sin\frac{\beta(L-l_1-l_3)}{2}}{\cos\frac{\beta L}{2}},\quad \frac{\prod_{p=1}^{3}\sin(\beta l_p)}{\cos\frac{\beta L}{2}}\cong 0
\end{gathered}\tag{28}$$

Eq. (27) can then rewritten as

$$\begin{aligned}
\tan\frac{\beta L}{2}-\left[\frac{\beta L}{2}-\frac{4}{\lambda^2}\left(\frac{\beta L}{2}\right)^3\right]\cong\ &\frac{\left[\frac{\beta L}{2}-\frac{4}{\lambda^2}\left(\frac{\beta L}{2}\right)^3\right]\left\{\begin{array}{c}2\left[\sin\frac{\beta l_1}{2}\sin\frac{\beta(L-l_1)}{2}\cos^{-1}\left(\frac{\beta L}{2}\right)\right]^2\xi_1+2\left[\sin\frac{\beta l_3}{2}\sin\frac{\beta(L-l_3)}{2}\cos^{-1}\left(\frac{\beta L}{2}\right)\right]^2\xi_2\\ +4\sin\frac{\beta l_1}{2}\sin\frac{\beta(l_1+l_3)}{2}\sin\frac{\beta l_3}{2}\left[\sin\frac{\beta(L-l_1-l_3)}{2}\cos^{-1}\left(\frac{\beta L}{2}\right)\right]^2\xi_1\xi_2\end{array}\right\}}{\begin{array}{c}\tan\frac{\beta L}{2}+2\sin\frac{\beta l_1}{2}\sin\frac{\beta(L-l_1)}{2}\cos^{-1}\left(\frac{\beta L}{2}\right)\xi_1+2\sin\frac{\beta l_3}{2}\sin\frac{\beta(L-l_3)}{2}\cos^{-1}\left(\frac{\beta L}{2}\right)\xi_2\\ +4\sin^{-1}\left(\frac{\beta L}{2}\right)\sin\frac{\beta l_1}{2}\sin\frac{\beta l_2}{2}\sin\frac{\beta l_3}{2}\tan\frac{\beta L}{2}\xi_1\xi_2\end{array}}
\end{aligned}\tag{29}$$

For $l_1 \ll L$ and $l_3 \ll L$, the following approximations can be introduced

$$\begin{gathered}
\sin\frac{\beta(L-l_1)}{2}\cong\sin\frac{\beta L}{2},\quad \sin\frac{\beta(L-l_3)}{2}\cong\sin\frac{\beta L}{2}\\
\sin\frac{\beta l_2}{2}\cong\sin\frac{\beta L}{2},\quad \frac{\sin\frac{\beta(L-l_1)}{2}}{\cos\frac{\beta L}{2}}\cong\tan\frac{\beta L}{2}-\frac{\beta l_1}{2}\\
\frac{\sin\frac{\beta(L-l_3)}{2}}{\cos\frac{\beta L}{2}}\cong\tan\frac{\beta L}{2}-\frac{\beta l_3}{2}\\
\frac{\sin\frac{\beta(L-l_1-l_3)}{2}}{\cos\frac{\beta L}{2}}\cong\tan\frac{\beta L}{2}-\frac{\beta(l_1+l_3)}{2}
\end{gathered}\tag{30}$$

Meanwhile, the left-hand side of Eq. (29) is linearized around the undamped wavenumber β_n^0, i.e.,

$$\begin{aligned}
&\tan\frac{\beta_n^0 L}{2}-\left[\frac{\beta_n^0 L}{2}-\frac{4}{\lambda^2}\left(\frac{\beta_n^0 L}{2}\right)^3\right]\\
&\cong\left[\tan^2\left(\frac{\beta_n^0 L}{2}\right)+\frac{12}{\lambda^2}\left(\frac{\beta_n^0 L}{2}\right)^2\right]\frac{\Delta\beta_n L}{2}
\end{aligned}\tag{31}$$

With these manipulations, the expression for the complex wavenumber increment is obtained from Eq. (29) as follows

$$\Delta\beta_n \cong \frac{\beta_n^0}{L} \frac{\begin{array}{c}\beta_n^0 l_1^2\left(\tan\frac{\beta_n^0 L}{2}-\frac{\beta_n^0 l_1}{2}\right)^2\xi_1+\beta_n^0 l_3^2\left(\tan\frac{\beta_n^0 L}{2}-\frac{\beta_n^0 l_3}{2}\right)^2\xi_2 \\ +(\beta_n^0)^2 l_1(l_1+l_3)l_3\left[\tan\frac{\beta_n^0 L}{2}-\frac{\beta_n^0(l_1+l_3)}{2}\right]^2\xi_1\xi_2\end{array}}{\left[\tan^2\left(\frac{\beta_n^0 L}{2}\right)+\frac{12}{\lambda^2}\left(\frac{\beta_n^0 L}{2}\right)^2\right](1+\beta_n^0 l_1\xi_1+\beta_n^0 l_3\xi_2+\beta_n^0 l_1\beta_n^0 l_3\xi_1\xi_2)} \tag{32}$$

Further using the non-dimensional parameters, Eq. (32) is written as

$$\Delta\beta_n \cong \frac{\beta_n^0}{L} \frac{\begin{array}{c}l_1(\bar{k}+\mathrm{i}\kappa)\left(\tan\frac{\beta_n^0 L}{2}-\frac{\beta_n^0 l_1}{2}\right)^2+l_3(\bar{K}+\mathrm{i}\varphi\bar{K})\left(\tan\frac{\beta_n^0 L}{2}-\frac{\beta_n^0 l_3}{2}\right)^2 \\ +(l_1+l_3)(\bar{k}+\mathrm{i}\kappa)(\bar{K}+\mathrm{i}\varphi\bar{K})\left[\tan\frac{\beta_n^0 L}{2}-\frac{\beta_n^0(l_1+l_3)}{2}\right]^2\end{array}}{\left[1+(\bar{k}+\mathrm{i}\kappa)+(\bar{K}+\mathrm{i}\varphi\bar{K})+(\bar{k}+\mathrm{i}\kappa)(\bar{K}+\mathrm{i}\varphi\bar{K})\right]\left[\tan^2\left(\frac{\beta_n^0 L}{2}\right)+\frac{12}{\lambda^2}\left(\frac{\beta_n^0 L}{2}\right)^2\right]} \tag{33}$$

Correspondingly, the damping ratio is obtained as

$$\zeta_n \cong \frac{1}{L} \frac{\begin{array}{c}\left\{\begin{array}{l}l_1\kappa\left(\tan\frac{\beta_n^0 L}{2}-\frac{\beta_n^0 l_1}{2}\right)^2+l_3\varphi\bar{K}\left(\tan\frac{\beta_n^0 L}{2}-\frac{\beta_n^0 l_3}{2}\right)^2 \\ +(l_1+l_3)(\bar{k}\varphi\bar{K}+\kappa\bar{K})\left[\tan\frac{\beta_n^0 L}{2}-\frac{\beta_n^0(l_1+l_3)}{2}\right]^2\end{array}\right\}(1+\bar{k}+\bar{K}+\bar{k}\bar{K}-\kappa\varphi\bar{K}) \\ -\left\{\begin{array}{l}l_1\bar{k}\left(\tan\frac{\beta_n^0 L}{2}-\frac{\beta_n^0 l_1}{2}\right)^2+l_3\bar{K}\left(\tan\frac{\beta_n^0 L}{2}-\frac{\beta_n^0 l_3}{2}\right)^2 \\ +(l_1+l_3)(\bar{k}\bar{K}-\kappa\varphi\bar{K})\left[\tan\frac{\beta_n^0 L}{2}-\frac{\beta_n^0(l_1+l_3)}{2}\right]^2\end{array}\right\}(\kappa+\varphi\bar{K}+\bar{k}\varphi\bar{K}+\kappa\bar{K})\end{array}}{\left[(1+\bar{k}+\bar{K}+\bar{k}\bar{K}-\kappa\varphi\bar{K})^2+(\kappa+\varphi\bar{K}+\bar{k}\varphi\bar{K}+\kappa\bar{K})^2\right]\left[\tan^2\left(\frac{\beta_n^0 L}{2}\right)+\frac{12}{\lambda^2}\left(\frac{\beta_n^0 L}{2}\right)^2\right]}, \quad n=1,3,\cdots \tag{34}$$

Define the reduction factor owing to the cable sag effect as Krenk and Nielsen (2002)

$$R_p=\left(\tan\frac{\beta_n^0 L}{2}-\frac{\beta_n^0 l_p}{2}\right)^2\Bigg/\left[\tan^2\left(\frac{\beta_n^0 L}{2}\right)+\frac{12}{\lambda^2}\left(\frac{\beta_n^0 L}{2}\right)^2\right]$$

with the cable element index $p=1,3$. As $l_1 \ll L$ and $l_3 \ll L$. The reduction factor is not sensitive to the damper location (as will be shown in Fig. 2). Hence, further using the following approximation.

$$(l_1+l_3)\frac{\left[\tan\left(\frac{\beta_n^0 L}{2}\right)-\frac{\beta_n^0(l_1+l_3)}{2}\right]^2}{\tan\left(\frac{\beta_n^0 L}{2}\right)+\frac{12}{\lambda^2}\left(\frac{\beta_n^0 L}{2}\right)^2} \cong l_1R_1+l_3R_3$$

One can obtain a simpler expression as

$$\zeta_n \cong \frac{\kappa}{(1+\bar{k})^2+\kappa^2}\frac{l_1}{L}R_1+\frac{\varphi\bar{K}}{(1+\bar{K})^2+\varphi^2\bar{K}^2}\frac{l_3}{L}R_3 \quad n=1,3,\cdots \tag{35}$$

The preceding asymptotic expression for modal damping has two parts, respectively representing the contribution from the two dampers when installed separately. For symmetric modes, the right-hand side of Eq. (35) includes the reduction factor due to the influence of the cable sag, as derived by Krenk and Nielsen (2002). The maximum modal damping ratio in the cable is achieved when each of the dampers is respectively tuned to the optimal condition, that is

$$\kappa_{\mathrm{opt}} \cong 1+\bar{k},\ \bar{K}_{\mathrm{opt}}=\frac{1}{\sqrt{1+\varphi^2}} \text{ and}$$
$$\zeta_{n,\mathrm{opt}} \cong 0.5R_1\frac{1}{1+\bar{k}}\frac{l_1}{L}+0.5R_2\frac{\varphi}{1+\sqrt{1+\varphi^2}}\frac{l_3}{L}$$

3.1.3 Parametric analysis

The influence of cable sag: Note that in the cable-stayed bridges the value of λ^2 is normally less than 3 (Tabatabai and Mehrabi 2000). For example, $\lambda^2 \cong 2$ for the longest cables of the Sutong bridge. The longest cable of Dubai creek tower (under construction) is of more than 700 m, and approximately $\lambda^2 \cong 10$. In this context, the range of the Irvine parameter is considered to be $\lambda^2 \cong 0\sim20$ for parametric analysis. The reduction factor R_p for the first four vibration modes ($n=1\sim4$) are plotted in Fig. 2 for $\lambda^2 \cong 0\sim20$. For the antisymmetric modes ($n=2,4,\cdots$), the Irvine parameter λ^2 does not affect R_p ($R_p=1$). For the symmetric modes ($n=1,3,\cdots$), the influence of sag must be considered, especially for the first symmetric mode (Krenk and Nielsen 2002). It is known that the cable sag modifies the mode shape of symmetric cable modes. Particularly, relative cable motion near cable ends is reduced, such that less energy can be dissipated when the damper is installed near the cable end. This influence becomes more pronounced as the Irvine parameter increases (in the range of $\lambda^2 \cong 0\sim20$) and as the damper is installed closer to the cable end, as showed in Fig. 2.

Analysis of the parameters of dampers: Fig. 3 shows the cable damping curves when the external damper with intrinsic stiffness $\bar{k}=0.1$ is installed at $l_1/L=0.02$ and the internal HDR damper with different loss factors and optimal stiffness is installed at $l_3/L=0.02$ but close to the other end, for the first and second cable modes. Eqs. (25) and (35) show that the total modal damping effect is approximately the sum of the contributions from the dampers when installed separately, as also seen in Fig. 3.

Therefore, when considering cable sag, the damping effect of two dampers installed respectively close to the two

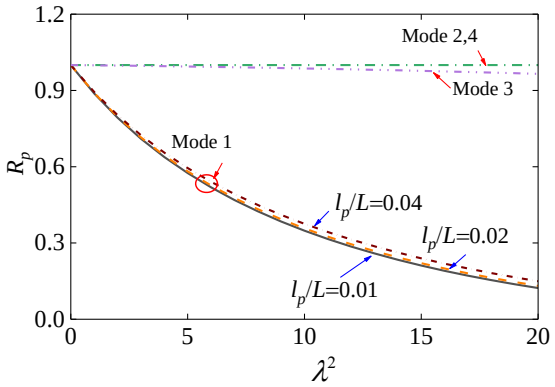

Fig. 2 Variation of the reduction factor due to the influence of cable sag

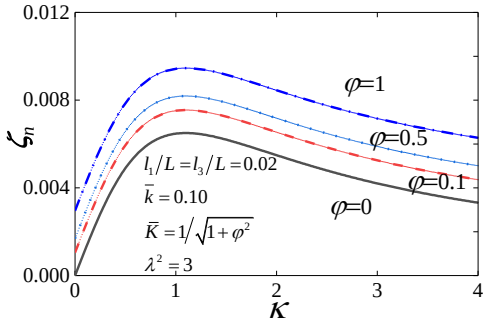

(a) n = 1

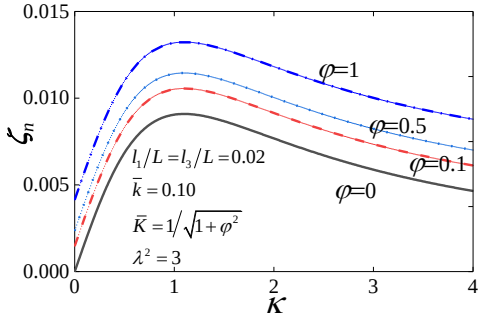

(b) n = 2

Fig. 3 Modal damping versus the viscous coefficient of the external damper of a cable with both internal and external dampers

cable ends can still be appreciated by analyzing the cable with each of the dampers separately. Fig. 3 also suggests a feasible solution to supplement additional damping when the damping provided by the external damper near the cable-deck anchorage is insufficient due to the sag effect and the damper stiffness, i.e., by installing an HDR damper near the cable-pylon anchorage.

Figs. 4-5 show the damping of a shallow cable respectively attached with an external damper and an internal damper. Consider that the dampers are installed at $l_p/L = 0.02$ and the cable sag is $\lambda^2 = 3$. Fig. 4(a) shows the cable damping curves of the antisymmetric modes when the viscous damper with different values of the intrinsic stiffness, i.e., $\bar{k} = 0,\ 0.10,\ 0.50, 1.00$. Fig. 4(b)

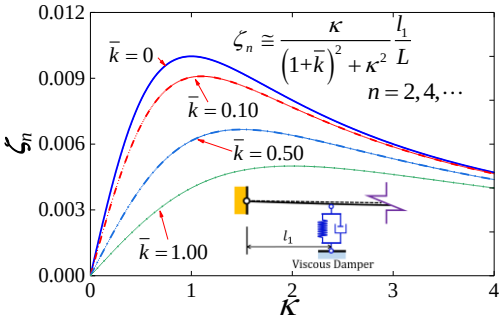

(a) Nearly antisymmetric vibrations

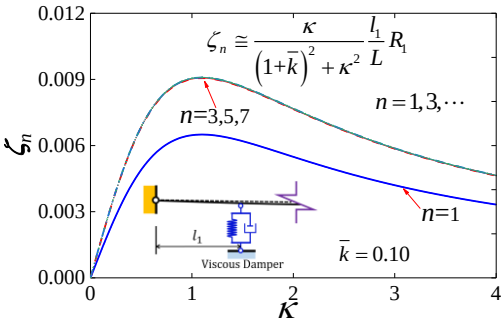

(b) Nearly symmetric vibrations

Fig. 4 Modal damping of a cable with a single viscous damper ($l_1/L = 0.02, \lambda^2 = 3$) both internal and external dampers

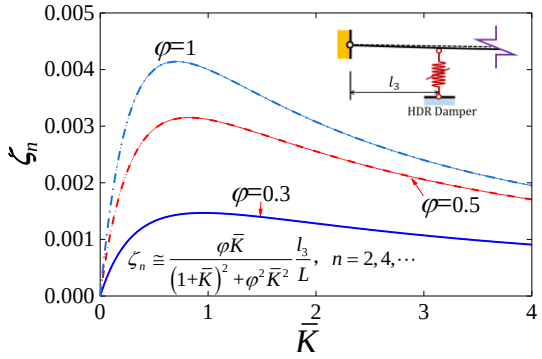

(a) Nearly antisymmetric vibrations

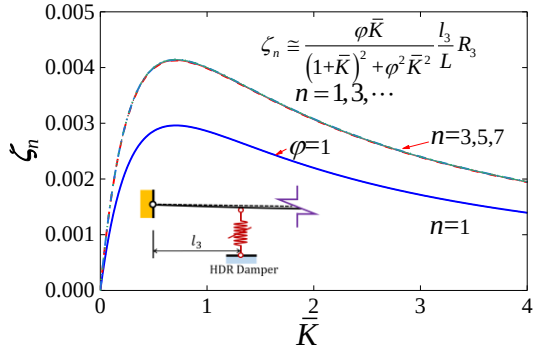

(b) Nearly symmetric vibrations

Fig. 5 Modal damping of a cable with a single HDR damper ($l_3/L = 0.02, \lambda^2 = 3$)

shows the cable damping curves of the symmetric modes

when the intrinsic stiffness parameter of the viscous damper is $\bar{k} = 0.10$. Fig. 5(a) shows the cable damping curves of the antisymmetric modes when the loss factor of the HDR damper varies, i.e., $\varphi = 0.3, 0.5, 1.0$. Fig. 5(b) shows the cable damping curves of the symmetric modes when the loss factor of the HDR damper is $\varphi = 1.0$.

From Fig. 4, it is seen that the stiffness of the viscous damper has a great influence on the damping effect of the viscous damper. The reduction effects of damper stiffness and cable sag should be considered in the design of viscous damper, especially for the first symmetric mode vibration. Fig. 5 indicates that the loss factor of HDR damper determines the maximum damping achievable. With the development of high-damping rubber materials, the loss factor of HDR damper can reach a value larger than 1.0. Hence, the HDR damper can be used for vibration reduction of medium length cables. Besides, it is a feasible countermeasure to improve cable damping by installing an HDR damper inside the guide pipe of the cable-pylon anchorage, when the external damper between the cable and the bridge deck is insufficient.

3.2 Dampers at the same end

3.2.1 Nearly antisymmetric modes

When the viscous damper and the HDR damper are installed at the same end, the HDR damper is closer to the cable end, namely $l_2 \ll L$ and $l_3 \ll L$. The distance between the external damper and the nearer cable anchorage is denoted by $l_1' = L - l_1 = l_2 + l_3$. Eq. (16) can be reduced to the following form using the similar approximations as used previously, as

$$\tan\frac{\beta L}{2} \cong \frac{\frac{1}{2}\sin^2[\beta(l_2+l_3)]\xi_1 + \frac{1}{2}\sin^2(\beta l_3)\xi_2 - \frac{1}{2}\sin(\beta l_1)\sin(\beta l_2)\sin(\beta l_3)\xi_1\xi_2}{1+\sin[\beta(l_2+l_3)]\cos^2\left[\frac{\beta(l_2+l_3)}{2}\right]\xi_1 + \sin(\beta l_3)\cos^2\left(\frac{\beta l_3}{2}\right)\xi_2 + \cos^2\left(\frac{\beta l_1}{2}\right)\sin(\beta l_2)\sin(\beta l_3)\xi_1\xi_2} \tag{36}$$

Further using the approximations for $l_2 \ll L$ and $l_3 \ll L$ leads to

$$\Delta\beta_n \cong \frac{\beta_n^0}{L}\frac{\beta_n^0(l_2+l_3)^2\xi_1 + \beta_n^0(l_3)^2\xi_2 + l_2\beta_n^0 l_3\beta_n^0(l_2+l_3)\xi_1\xi_2}{1+\beta_n^0(l_2+l_3)\xi_1 + \beta_n^0 l_3\xi_2 + \beta_n^0 l_2\beta_n^0 l_3\xi_1\xi_2} \quad n = 2,4,\cdots \tag{37}$$

For the dampers at the same end, the following non-dimensional parameters are defined as

$$\bar{k} = \frac{k(l_2+l_3)}{H} = \frac{kl_1'}{H}, \quad \kappa = \bar{c}(l_2+l_3)\beta_n^0 = \bar{c}l_1'\beta_n^0$$

Note the differences in the definitions of these non-dimensional parameters as compared to those in the previous case. Eq. (37) thus becomes

$$\Delta\beta_n \cong \frac{\beta_n^0}{L}\frac{(l_2+l_3)(\bar{k}+\mathrm{i}\kappa) + l_3(\bar{K}+\mathrm{i}\varphi\bar{K}) + l_2(\bar{k}+\mathrm{i}\kappa)(\bar{K}+\mathrm{i}\varphi\bar{K})}{1+(\bar{k}+\mathrm{i}\kappa) + (\bar{K}+\mathrm{i}\varphi\bar{K}) + l_2(l_2+l_3)^{-1}(\bar{k}+\mathrm{i}\kappa)(\bar{K}+\mathrm{i}\varphi\bar{K})} \tag{38}$$

Finally, the damping ratio is given as

$$\zeta_n \cong \frac{l_2+l_3}{L}\frac{[\kappa + l_3(l_2+l_3)^{-1}\varphi\bar{K} + l_2(l_2+l_3)^{-1}(\bar{k}\varphi\bar{K}+\kappa\bar{K})][1+\bar{k}+\bar{K}+l_2(l_2+l_3)^{-1}(\bar{k}\bar{K}-\kappa\varphi\bar{K})]}{-[\bar{k}+l_3(l_2+l_3)^{-1}\bar{K} + l_2(l_2+l_3)^{-1}(\bar{k}\bar{K}-\kappa\varphi\bar{K})][\kappa+\varphi\bar{K}+l_2(l_2+l_3)^{-1}(\bar{k}\varphi\bar{K}+\kappa\bar{K})]} \quad n = 2,4,\cdots \tag{39}$$

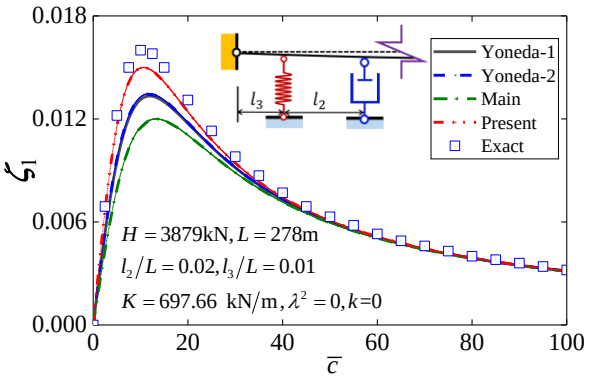

Fig. 6 Comparison of the damping curves obtained via different methods

3.2.2 Nearly symmetric modes

Like the simplification from Eq. (26) to Eq. (30), and considering $l_2 \ll L$ and $l_3 \ll L$, Eq. (16) can be transformed into the following form

$$\begin{aligned}&\tan\frac{\beta L}{2} - \left[\frac{\beta L}{2} - \frac{4}{\lambda^2}\left(\frac{\beta L}{2}\right)^3\right] \\ &\frac{1}{2}[\beta(l_2+l_3)]^2\left[\tan\frac{\beta L}{2} - \frac{\beta(l_2+l_3)}{2}\right]^2\xi_1 + \frac{1}{2}(\beta l_3)^2\left(\tan\frac{\beta L}{2} - \frac{\beta l_3}{2}\right)^2\xi_2 \\ &+\frac{1}{2}\beta l_3\beta(l_2+l_3)\beta l_2\left[\tan\frac{\beta L}{2} - \frac{\beta(l_2+l_3)}{2}\right]^2\xi_1\xi_2 \\ \cong\ &\frac{}{1+\beta(l_2+l_3)\xi_1 + \beta l_3\xi_2 + \beta l_2\beta l_3\xi_1\xi_2}\end{aligned} \tag{40}$$

Using the non-dimensional damper parameters, Eq. (40) becomes

$$\begin{aligned}\Delta\beta_n \cong\ &\frac{\beta_n^0}{L}\times\left[(l_2+l_3)\left[\tan\frac{\beta_n^0 L}{2} - \frac{\beta_n^0(l_2+l_3)}{2}\right]^2(\bar{k}+\mathrm{i}\kappa)\right. \\ &+l_3\left(\tan\frac{\beta_n^0 L}{2} - \frac{\beta_n^0 l_3}{2}\right)^2(\bar{K}+\mathrm{i}\varphi\bar{K}) + l_2\left[\tan\frac{\beta_n^0 L}{2}\right. \\ &\left.\left.-\frac{\beta_n^0(l_2+l_3)}{2}\right]^2(\bar{k}+\mathrm{i}\kappa)(\bar{K}+\mathrm{i}\varphi\bar{K})\right] / \\ &\left[\left[\tan^2\left(\frac{\beta_n^0 L}{2}\right) + \frac{12}{\lambda^2}\left(\frac{\beta_n^0 L}{2}\right)^2\right][1+(\bar{k}+\mathrm{i}\kappa)+(\bar{K}+\mathrm{i}\varphi\bar{K})\right. \\ &\left.+l_2(l_2+l_3)^{-1}(\bar{k}+\mathrm{i}\kappa)(\bar{K}+\mathrm{i}\varphi\bar{K})\right]\end{aligned} \tag{41}$$

Recall the definition of the reduction factor and in this case for the external damper define

$$R_1' = \left[\tan\frac{\beta_n^0 L}{2} - \frac{\beta_n^0(l_2+l_3)}{2}\right]^2 \Bigg/ \left[\tan^2\left(\frac{\beta_n^0 L}{2}\right) + \frac{12}{\lambda^2}\left(\frac{\beta_n^0 L}{2}\right)^2\right]$$

Then, the damping ratio is expressed as

$$\zeta_n \cong \frac{l_2+l_3}{L}\frac{\left[\kappa R_1' + l_3(l_2+l_3)^{-1}\varphi\bar{K}R_3 + l_2(l_2+l_3)^{-1}\left(\bar{k}\varphi\bar{K}+\kappa\bar{K}\right)R_1'\right]\left[1+\bar{k}+\bar{K}+l_2(l_2+l_3)^{-1}\left(\bar{k}\bar{K}-\kappa\varphi\bar{K}\right)\right]}{\left[1+\bar{k}+\bar{K}+l_2(l_2+l_3)^{-1}\left(\bar{k}\bar{K}-\kappa\varphi\bar{K}\right)\right]^2+\left[\kappa+\varphi\bar{K}+l_2(l_2+l_3)^{-1}\left(\bar{k}\varphi\bar{K}+\kappa\bar{K}\right)\right]^2} \quad (42)$$
$$n = 1,3,\cdots$$

3.2.3 Parametric analysis

The case of a spring and a viscous damper: When the loss factor φ is zero, the HDR damper is a spring with a stiffness $\bar{K}$, Eq. (39) can be rewritten into the following form

$$\zeta_n \cong \frac{l_2+l_3}{L}\frac{\kappa+2l_2(l_2+l_3)^{-1}\kappa\bar{K}+[l_2(l_2+l_3)^{-1}-l_3l_2(l_2+l_3)^{-2}]\kappa\bar{K}^2}{\left[1+\bar{k}+\bar{K}+l_2(l_2+l_3)^{-1}\bar{k}\bar{K}\right]^2+[\kappa+l_2(l_2+l_3)^{-1}\kappa\bar{K}]^2}, \qquad n = 2,4,\cdots \quad (43)$$

For a small value of λ^2, $\tan\frac{\beta_n^0 L}{2}-\frac{\beta_n^0(l_2+l_3)}{2}\cong\tan\frac{\beta_n^0 L}{2}-\frac{\beta_n^0 l_3}{2}$. Eq. (42) can further be rewritten into the following form

$$\zeta_n \cong \frac{l_2+l_3}{L}\frac{\kappa+2l_2(l_2+l_3)^{-1}\kappa\bar{K}+[l_2(l_2+l_3)^{-1}-l_3l_2(l_2+l_3)^{-2}]\kappa\bar{K}^2}{\left[1+\bar{k}+\bar{K}+l_2(l_2+l_3)^{-1}\bar{k}\bar{K}\right]^2+[\kappa+l_2(l_2+l_3)^{-1}\kappa\bar{K}]^2}R_1', \qquad n = 1,3,\cdots \quad (44)$$

In previous studies, the bushing has been considered as a spring (Main and Jones 2003, Takano *et al.* 1997). Yoneda *et al.* (1995) proposed two equivalent methods (see Appendix A) for analyzing the effect of the bushing on the damper performance. Main and Jones (2003) derived an explicit asymptotic expression for the effective damper location (see Appendix B). Fig. 6 displays the comparison of these methods to the present formula, where a cable has a length of $L = 278$ m, the cable tension is $H = 3879$ kN, the cable sag parameter $\lambda^2 = 0$, a spring with stiffness $K = 697.66$ kN/m is installed at $l_3/L = 0.01$, and a viscous damper with the intrinsic stiffness $\bar{k} = 0$ is installed at $l_2/L = 0.02$. The numerical solution of Eq. (16) is regarded as the exact solution. The comparison shows that the asymptotic expression in the present study gives the most accurate estimate, the results obtained by using the two methods proposed by Yoneda *et al.* (1995) are almost the same, and the result from Main and Jones (2003) is more conservative.

To derive the asymptotic expression for the optimal damping parameter of the viscous damper, from Eq. (43) or (44), one finds

$$\kappa_{\text{opt}} = \bar{k} + \frac{1+\bar{K}}{1+l_2(l_2+l_3)^{-1}\bar{K}} \quad (45)$$

by letting $\partial\zeta_n/\partial\kappa = 0$. Substituting κ_{opt} into Eqs. (39) and (42) or Eqs. (43) and (44), leads to the maximum modal damping.

Fig. 7 shows the cable damping curves when the internal damper (spring) with different stiffness $\bar{K}$ is installed at $l_3/L = 0.01$ and the external damper with the intrinsic stiffness $\bar{k} = 0.10$ is installed at $l_2/L = 0.02$, for the first and second cable modes. Fig. 7 shows the apparent influence of the internal damper on the effectiveness of external damper for cable vibration mitigation. The internal damper (spring) reduces the maximum attainable damping ratio in each mode and increases the corresponding optimal value of the external damper coefficient, as implied by Eq. (45).

The case of an HDR damper and a viscous damper: This section further analyzes the dependence of the modal damping on the loss factor of the HDR damper for $\varphi = 0\sim1$. Fig. 8 shows the damping curves along with the parameter κ. It is seen that a nonzero loss factor would further reduce the maximum attainable damping ratio of the

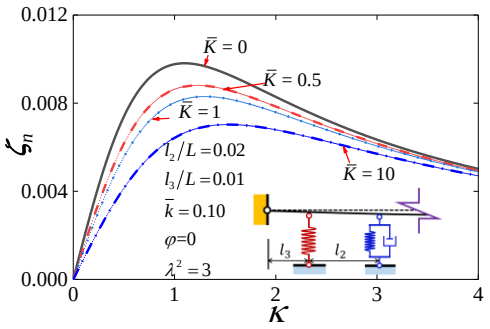

(a) $n = 1$

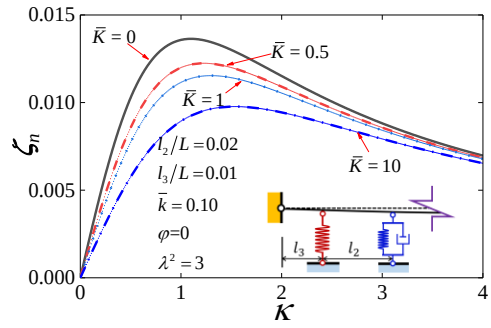

(b) $n = 2$

Fig. 7 Dependence of modal damping on spring stiffness $\bar{K}$ and the damper coefficient parameter κ

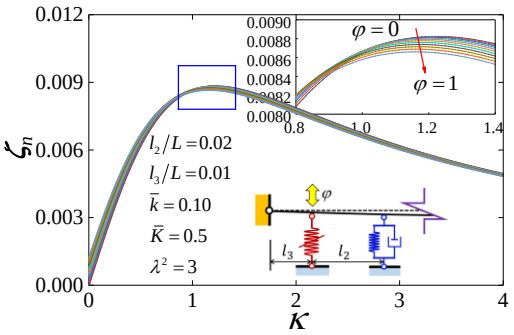

(a) n = 1

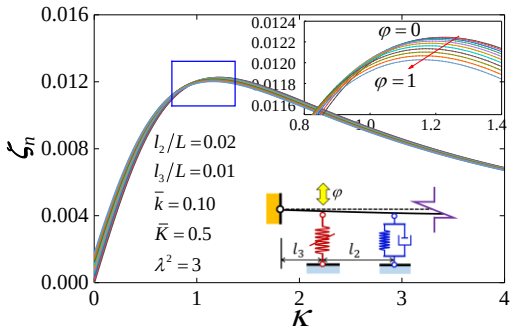

(b) n = 2

Fig. 8 Dependence of modal damping on the loss factor of the HDR

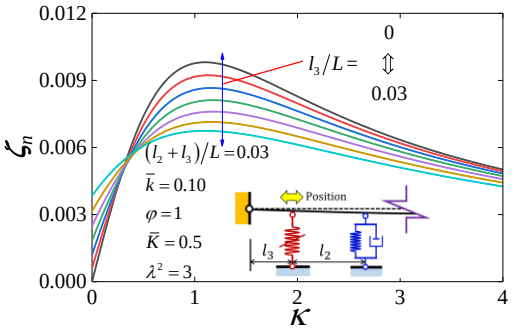

(a) n = 1

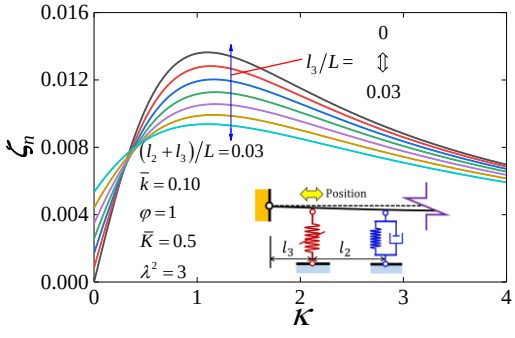

(b) n = 2

Fig. 9 Dependence of modal damping on the position of the HDR damper

cable. The negative effect is nevertheless very small and negligible, as displayed by the closeup view in Fig. 8.

Fig. 9 shows the dependence of modal damping on the

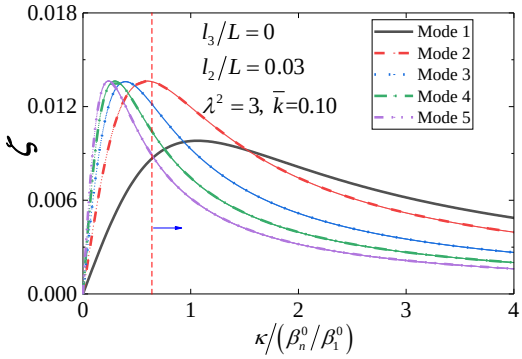

(a) Design of the viscous damper targeting multiple cable modes

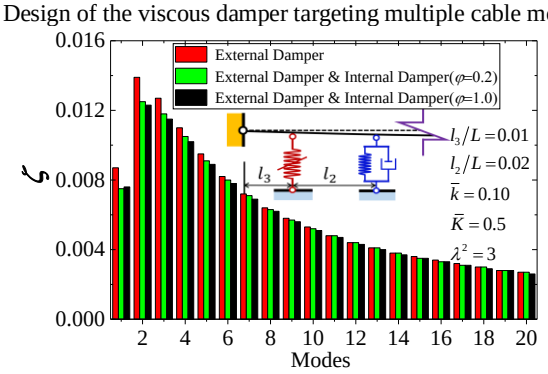

(b) Multimode damping ratios of a cable with a single external damper and with both external and internal dampers

Fig. 10 Multimode damping effects of the dampers on the cable

HDR installation position. When the damping coefficient of the viscous damper is small (the left side of the intersection of damping curves), the HDR damper plays a major role in providing damping, and a larger installation position of the HDR damper leads to increase in modal damping. If the damping coefficient of the viscous damper is already large (the right side of the intersection of damping curves), the presence of the HDR damper harms the performance of the viscous damper, and this effect becomes more pronounced when the HDR is closer to the viscous damper.

In practical design, the parameters of an external damper are determined according to the damping curves of the first several cable modes (Weber *et al*. 2009). For example, as shown in Fig. 10(a), the first five modes are considered to optimize the damping coefficient of a viscous damper with intrinsic stiffness $\bar{k}=0.10$ installed at $(l_2+l_3)/L=0.03$, where the Irvine parameter of the cable is set as $\lambda^2=3$, the optimal damping coefficient is found to be $\kappa/(\beta_n^0/\beta_1^0)\cong 0.65$. With these damper parameters determined, Fig. 10(b) plots the modal damping ratios of the first 20 modes of the cable. To appreciate the influence of the internal damper on the performance of the external damper, an internal damper with stiffness $\bar{K}=0.5$ and two different loss factors (0.2 and 1.0 respectively) is considered being installed at $l_3/L=0.01$. Correspondingly, the damping ratios of the cable with the two dampers are shown in Fig. 10(b). Note that the approximate solution can only guarantee the accuracy of cable modal damping ratios for the first several modes (Krenk 2000). The results in Fig.

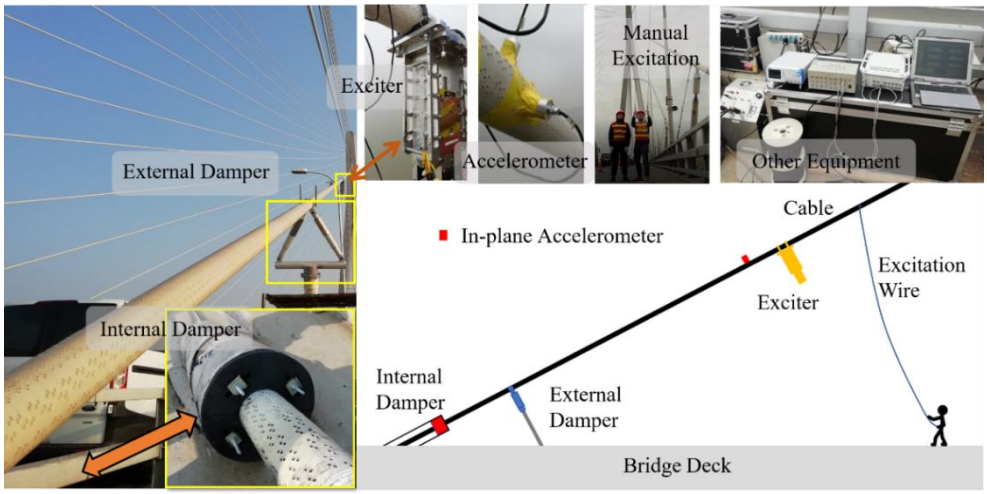

Fig. 11 The experiment setup

10(b) are computed numerically. As shown in Fig. 10(b), considering multimode vibration control of the cable, the internal damper impairs the effect of the external damper for lower modes. For higher modes, the influence of the internal damper system damping gradually decreases. Comparing the impacts of the internal damper with two different loss factors (0.2 and 1.0 respectively) on the external damper, the negative effect of an internal damper with a larger loss factor on the external damper is more significant except for the first mode. The internal damper stiffness could significantly reduce the damping achieved by the external damper, which has been interpreted as a reduction of the effective distance between the external damper and the cable end or an increase in intrinsic stiffness of the external damper (Yoneda *et al*. 1995, Main and Jones 2003). The energy dissipation capacity of the internal damper can be interpreted as increasing damping coefficient of the external damper. As such, after the installation of the internal damper, the equivalent coefficient of the external damper is larger than the optimal one as indicated by the dashed line in Fig. 10(a). As seen from the damping curves in Fig. 10(a), increasing damping coefficient of the external damper decreases cable model damping ratio except for the first mode. It is also seen in Fig. 10(b) that the damping ratio decreases (except for the first mode) with increasing loss factor of the HDR damper.

3.3 Discussion and remarks

The theoretical analysis shows that the total damping effect provided by the dampers installed at opposite ends is about the sum of separate contributions of the dampers, which extend the conclusion in the previous studies concerning taut cables and ideally viscous dampers (Caracoglia and Jones 2007, Hoang and Fujino 2008). For multimode cable vibration control, the parameters of the external damper can be optimized according to the first several cable modes (Weber *et al*. 2009). For the internal damper (HDR damper), the loss factor should be as large as possible, and the stiffness of damper should be optimized according to the loss factor as $\bar{K}_{\text{opt}} = 1/\sqrt{1+\varphi^2}$. A larger installation distance is essential to improve the damping effect, and the length of the guide pipe should be designed accordingly. For long cables, the sag effect and the damper inherent stiffness impair the damper control performance on the lower modes of the cable vibration. Installation of internal dampers near the bridge tower side can improve the damping in such cases.

To reduce cable bending stresses near the anchorages, the neoprene rubber bushings, are desired to be installed on stay cables inside the steel guide pipes. From the theoretical analysis of this study, the additional transverse stiffness of the bushings could significantly reduce the external damper effectiveness, and improving the energy dissipation capacity of the internal dampers is insignificant for multimode vibration control of the cable. Therefore, in the premise of fulfilling the design requirements for reducing the bending stress, the stiffness of internal damper should be as small as possible, and the installation distance should be as far away from the external damper as possible. Compared with the installation of dampers at the opposite ends, the energy dissipation of the internal damper is not so important for cable vibration control in the lower vibration modes. But for some higher vibration modes, when the external damper is located on the node of the vibration modes, the internal HDR damper with greater loss factor can help reduce the vibrations.

4. Experimental study

For validation of the theoretical analysis in section 3.2, experiments have been carried out on a cable of the Sutong Bridge in China. The length of the tested cable is L = 454.1 m, the mass per unit length is m = 77.65 kg/m, the axial tension is H = 5099 kN, and the Irvine parameter is $\lambda^2 = 1.5$. A viscous damper is installed about 10.689 m away from the cable anchorage point. The damping coefficient of the viscous damper is about c = 90 kN.s/m (the equivalent coefficient for in-plane vibrations of the two viscous dampers shown in Fig. 11), which is optimized for the first eleven cable modes. The intrinsic stiffness of the

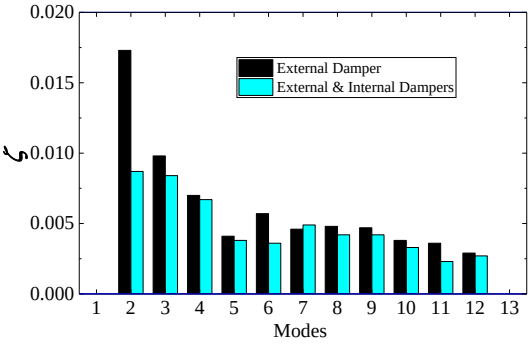

(a) Experimental results

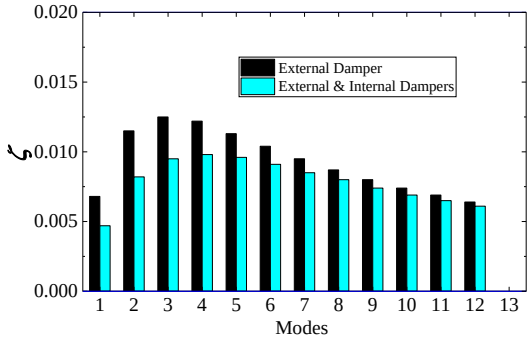

(b) Theoretical results

Fig. 12 Comparison of the measured and theoretical damping ratios

viscous damper is ignored based on laboratory test results. The internal damper is an HDR damper installed at the end of the steel cable guide pipe, about 3.987 m away from the cable anchorage point, the loss factor of HDR damper is about $\varphi = 0.20$, and the stiffness of HDR damper is about $K = 2000$ kN/m.

Field tests have been performed to measure the damping of the cable with only the external dampers and with both viscous and HDR dampers, respectively. The cable was excited to vibrate in a target mode, and then the vibration was left to decay freely after its amplitude reached a certain value. Modal damping of this mode was then computed from the free-decaying cable response. Fig. 11 demonstrates the testing scheme. Accelerometers were placed on the cable about 13 m above the bridge deck to measure cable accelerations during vibrations. For vibration excitation, an exciter was attached to the cable also about 13 m above the bridge deck. Steel wires were also used for manual excitations when the exciter was inadequate for exciting vibrations in lower-modes. Fig. 11 shows photos of the installed sensors and the exciter.

Fig. 12(a) illustrates the results of the field tests. For almost all modes, the cable modal damping decreases with the installation of the internal damper. Fig. 12(b) shows the corresponding theoretical results. Note that the measured cable inherent damping (about 0.05%) is added in the theoretical damping ratio. From Fig. 12(a), it is seen that the damping effect of the external damper (viscous damper) is reduced in the presence of the internal damper (HDR damper), which qualitatively agree with the theoretical results as shown in Fig. 12(b). However, quantitative discrepancies between the measured and the estimated damping ratios are observable for all the modes. The measured damping in mode 2 is particularly larger than the theoretical prediction mainly because of the unsuccessful vibration excitation (Chen *et al*. 2020). For the other modes, the theoretical damping ratios are larger than the respective measurements, which is attributed to the efficiency loss probably induced by the damper joints and nonlinear behaviors. The cable damping ratio of the fundamental mode was not measured due to the difficulty in exciting the cable vibrations in low frequencies. Hence, the damping ratio of the first cable mode is not shown in Fig. 12.

5. Conclusions

This paper presents a comprehensive theoretical analysis of a shallow cable with an external damper and an internal damper together with an experimental study for validation. The external damper is considered to be a viscous damper with intrinsic stiffness, and the internal damper is regarded as an HDR damper. The sag of the cable is considered. Asymptotic expressions are derived for modal damping ratio in cases of the dampers close to either the same cable end or the opposite cable ends. The following conclusions can be drawn.

• Considering intrinsic stiffness of the external damper and cable sag effect, when the dampers are installed at opposite ends of the cable, the total damping effect is still asymptotically the sum of the contributions from each of the dampers when installed separately. The maximum modal damping ratio of the cable is achieved when each damper is respectively tuned to the optimal condition. An internal damper installed near the bridge tower can compensate for efficiency loss of the external damper due to the damper stiffness and the sag effect. This strategy can be a feasible countermeasure for long cable vibration mitigation in practice.

• When the dampers are installed near the same cable end, the presence of the internal damper decreases the maximum attainable damping provided by the external damper for lower cable modes. Specifically, the transverse stiffness introduced by the internal damper significantly reduce the effectiveness of the external damper. The closer the internal damper is to the external damper, the greater the reduction effect is. The loss factor of the internal damper has pretty limited influences on the performance of the external damper for multimode cable vibration control. Therefore, the influence of the internal damper (or rubber bushings) on the effectiveness of external cable dampers should be evaluated in the damper design, using the accurate asymptotic expressions or the numerical method provided in this study.

• The results of the field tests are found to be qualitatively consistent with the theoretical results. The modal damping of the cable, for almost all tested modes, decrease after the installation of the internal damper.

Note that the paper mainly focuses on the in-plane vibrations of the cable. However, theoretical development in this study also applies to cable out-plane vibrations,

where the effect of cable sag is absent.

Acknowledgments

This study was partly supported by the National Natural Science Foundation of China (Grant nos. 51978506, 51608390), which is gratefully acknowledged.

References

Caracoglia, L. and Jones, N.P. (2007), "Damping of taut-cable systems: Two dampers on a single stay", *J. Eng. Mech.*, **133**(10), 1050-1060. https://doi.org/10.1061/(ASCE)0733-9399(2007)133:10(1050).

Carne, T.G. (1981), "Guy cable design and damping for vertical axis wind turbines", Technical Report No. SAND80-2669, Sandia National Laboratories, Albuquerque, Mexico.

Chen, L. and Sun, L. (2016), "Steady-state analysis of cable with nonlinear damper via harmonic balance method for maximizing damping", *J. Struct. Eng.*, **143**(2), 04016172. https://doi.org/10.1061/(ASCE)ST.1943-541X.0001645.

Chen, Z.Q., Wang, X.Y., Ko, J.M., Ni, Y.Q., Spencer Jr, B.F. and Yang, G. (2003), "MR damping system on Dongting lake cable-stayed bridge", *Proceedings of the Smart Structures and Materials 2003: Smart Systems and Nondestructive Evaluation for Civil Infrastructures*: *International Society for Optics and Photonics*, San Diego, USA, June. https://doi.org/10.1117/12.498072.

Chen, L., Sun, L. and Nagarajaiah, S. (2015), "Cable with discrete negative stiffness device and viscous damper: Passive realization and general characteristics", *Smart Struct. Syst., Int. J.*, **15**(3), 627-643. http://dx.doi.org/10.12989/sss.2015.15.3.627.

Chen, L., Sun, L. and Nagarajaiah, S. (2016), "Cable vibration control with both lateral and rotational dampers attached at an intermediate location", *J. Sound Vib.*, **377**, 38-57. https://doi.org/10.1016/j.jsv.2016.04.028.

Chen, L., Di, F., Xu, Y., Sun, L., Xu, Y. and Wang, L. (2020), "Multimode cable vibration control using a viscous-shear damper: Case studies on the Sutong bridge", *Struct. Control Health Monit.*, **27**(6), e2536. https://doi.org/10.1002/stc.2536.

Cu, V.H., Han, B. and Wang, F. (2015), "Damping of a taut cable with two attached high damping rubber dampers", *Struct. Eng. Mech., Int. J.*, **55**(6), 1261-1278. https://doi.org/10.12989/sem.2015.55.6.1261.

De Sá Caetano, E. (2007), *Cable Vibrations in Cable-stayed Bridges*, Zurich, Switzerland.

Duan, Y., Ni, Y.Q., Zhang, H., Spencer Jr, B.F., Ko, J.M. and Dong, S. (2019a), "Design formulas for vibration control of sagged cables using passive MR dampers", *Smart Struct. Syst., Int. J.*, **23**(6), 537-551. https://doi.org/10.12989/sss.2019.23.6.537.

Duan, Y., Ni, Y.Q., Zhang, H., Spencer Jr, B.F., Ko, J.M. and Fang, Y. (2019b), "Design formulas for vibration control of taut cables using passive MR dampers", *Smart Struct. Syst., Int. J.*, **23**(6), 521-536. https://doi.org/10.12989/sss.2019.23.6.521.

Fujino, Y. and Hoang, N. (2008), "Design formulas for damping of a stay cable with a damper", *J. Struct. Eng.*, **134**(2), 269-278. https://doi.org/10.1061/(ASCE)0733-9445(2008)134:2(269).

Fujino, Y., Kichiro, K. and Tanaka, H. (2012), *Wind Resistant Design of Bridges in Japan*, Springer, Tokyo, Japan.

Hikami, Y. and Shiraishi, N. (1988), "Rain-wind induced vibrations of cables stayed bridges", *J. Wind Eng. Ind. Aerodyn.*, **29** (1-3), 409-418. https://doi.org/10.1016/0167-6105(88)90179-1.

Hoang, N. and Fujino, Y. (2007), "Analytical study on bending effects in a stay cable with a damper", *J. Eng. Mech.*, **133**(11), 1241-1246. https://doi.org/10.1061/(ASCE)0733-9399(2007)133:11(1241).

Hoang, N. and Fujino, Y. (2008), "Combined damping effect of two dampers on a stay cable", *J. Bridge. Eng.*, **13**(3), 299-303. https://doi.org/10.1061/(ASCE)1084-0702(2008)13:3(299).

Huang, Z., Hua, X., Chen, Z. and Niu, H. (2019), "Performance evaluation of inerter-based damping devices for structural vibration control of stay cables", *Smart Struct. Syst., Int. J.*, **23**(6), 615-626. https://doi.org/10.12989/sss.2019.23.6.615.

Irvine, H.M. (1981), *Cable Structures*, MIT Press, Cambridge, MA, USA.

Irvine, H.M. and Caughey, T.K. (1974), "The linear theory of free vibrations of a suspended cable", *Proc. R. Soc. A*, **341**(1626), 299-315. https://doi.org/10.1098/rspa.1974.0189.

Kovacs, I. (1982), "Zur frage der seilschwingungen und der seildämpfung", *Bautechnik*, **59**(10), 325-332. https://doi.org/view/1035863.

Krenk, S. (2000), "Vibrations of a taut cable with an external damper", *J. Appl. Mech.*, **67**(4), 772-776. https://doi.org/10.1115/1.1322037.

Krenk, S. and Nielsen, S.R. (2002), "Vibrations of a shallow cable with a viscous damper", *Proc. R. Soc. A*, **458**(2018), 339-357. https://doi.org/10.1098/rspa.2001.0879.

Lu, L., Duan, Y.F., Spencer Jr, B.F., Lu, X. and Zhou, Y. (2017), "Inertial mass damper for mitigating cable vibration", *Struct. Control Health Monit.*, **24**(10), e1986. https://doi.org/10.1002/stc.1986.

Lu, L., Fermandois, G.A., Lu, X., Spencer Jr, B.F., Duan, Y.F. and Zhou, Y. (2019), "Experimental evaluation of an inertial mass damper and its analytical model for cable vibration mitigation", *Smart Struct. Syst., Int. J.*, **23**(6), 589-613. https://doi.org/10.12989/sss.2019.23.6.589.

Main, J.A. (2002), "Modeling the vibrations of a stay cable with attached damper", Ph.D. Dissertation, Johns Hopkins University, Baltimore, USA.

Main, J.A. and Jones, N.P. (2002a), "Free vibrations of taut cable with attached damper. I: Linear viscous damper", *J. Eng. Mech.*, **128**(10), 1062-1071. https://doi.org/10.1061/(ASCE)0733-9399(2002)128:10(1062).

Main, J.A. and Jones, N.P. (2002b), "Free vibrations of taut cable with attached damper. II: Nonlinear damper", *J. Eng. Mech.*, **128**(10), 1072-1081. https://doi.org/10.1061/(ASCE)0733-9399(2002)128:10(1072).

Main, J.A. and Jones, N.P. (2003), "Influence of rubber bushings on stay-cable damper effectiveness", *Proceedings of Fifth International Symposium on Cable Dynamics*, Santa Margherita Ligure, Italy, September.

Main, J.A. and Jones, N.P. (2007), "Vibration of tensioned beams with intermediate damper. I: Formulation, influence of damper location", *J. Eng. Mech.*, **133**(4), 379-388. https://doi.org/10.1061/(ASCE)0733-9399(2007)133:4(369).

Matsumoto, M., Yagi, T., Shigemura, Y. and Tsushima, D. (2001), "Vortex-induced cable vibration of cable-stayed bridges at high reduced wind velocity", *J. Wind Eng. Ind. Aerodyn.*, **89**(7-8), 633-647. https://doi.org/10.1016/S0167-6105(01)00063-0.

Nakamura, A., Kasuga, A. and Arai, H. (1998), "The effects of mechanical dampers on stay cables with high-damping rubber", *Constr. Build. Mater.*, **12**(2-3), 115-123. https://doi.org/10.1016/S0950-0618(97)00013-5.

Nielsen, S.R. and Krenk, S. (2003), "Whirling motion of a shallow cable with viscous dampers", *J. Sound Vib.*, **265**(2), 417-435. https://doi.org/10.1016/S0022-460X(02)01455-4.

Pacheco, B.M., Fujino, Y. and Sulekh, A. (1993), "Estimation curve for modal damping in stay cables with viscous damper", *J. Struct. Eng.*, **119**(6), 1961-1979. https://doi.org/10.1061/(ASCE)0733-9445(1993)119:6(1961).

Sun, L. and Chen, L. (2015), "Free vibrations of a taut cable with a

general viscoelastic damper modeled by fractional derivatives", *J. Sound Vib.*, **335**, 19-33. https://doi.org/10.1016/j.jsv.2014.09.016.
Sun, L. and Huang, H. (2008), "Design, implementation and measurement of cable dampers for large cable-stayed bridges", *IABSE Congress Rep.*, **17**(16), 242-243.
Sun, L., Hong, D. and Chen, L. (2017), "Cables interconnected with tuned inerter damper for vibration mitigation", *Eng. Struct.*, **151**, 57-67. https://doi.org/10.1016/j.engstruct.2017.08.009.
Sun, L., Hong, D. and Chen, L. (2019a), "In-plane free vibrations of shallow cables with cross-ties", *Struct. Control Health Monit.*, **26**(10), e2421. https://doi.org/10.1002/stc.2421.
Sun, L., Xu, Y. and Chen, L. (2019b), "Damping effects of nonlinear dampers on a shallow cable", *Eng. Struct.*, **196**, 109305. https://doi.org/10.1016/j.engstruct.2019.109305.
Tabatabai, H. and Mehrabi, A.B. (2000), "Design of mechanical viscous dampers for stay cables", *J. Bridge Eng.*, **5**(2), 114-123. https://doi.org/10.1061/(ASCE)1084-0702(2000)5:2(114).
Takano, H., Ogasawara, M., Ito, N., Shimosato, T., Takeda, K. and Murakami, T. (1997), "Vibrational damper for cables of the Tsurumi Tsubasa bridge", *J. Wind Eng. Ind. Aerodyn.*, **69**, 807-818. https://doi.org/10.1016/S0167-6105(97)00207-9.
Uno, K., Kitagawa, S., Tsutsumi, H., Inoue, A. and Nakaya, S. (1991), "A simple method of designing cable vibration dampers of cable-stayed bridges", *J. Struct. Eng.*, **37** (1991), 789-798.
Wang, X.Y., Ni, Y.Q., Ko, J.M. and Chen, Z.Q. (2005), "Optimal design of viscous dampers for multimode vibration control of bridge cables", *Eng. Struct.*, **27**(5), 792-800. https://doi.org/10.1016/j.engstruct.2004.12.013.
Wang, Z.H., Xu, Y.W., Gao, H., Chen, Z.Q., Xu, K. and Zhao, S.B. (2019), "Vibration control of a stay cable with a rotary electromagnetic inertial mass damper", *Smart Struct. Syst., Int. J.*, **23**(6), 627-639. https://doi.org/10.12989/sss.2019.23.6.627.
Weber, F., Feltrin, G., Maślanka, M., Fobo, W. and Distl, H. (2009), "Design of viscous dampers targeting multiple cable modes", *Eng. Struct.*, **31**(11), 2797-2800. https://doi.org/10.1016/j.engstruct.2009.06.020.
Xu, Y.L. and Yu, Z. (1998a), "Vibration of inclined sag cables with oil dampers in cable-stayed bridges", *J. Bridge Eng.*, **3**(4), 194-203. https://doi.org/10.1061/(ASCE)1084-0702(1998)3:4(194).
Xu, Y.L. and Yu, Z. (1998b), "Mitigation of three-dimensional vibration of inclined sag cable using disrete oil dampers-II. Application", *J. Sound Vib.*, **214**(4), 675-693. https://doi.org/10.1006/jsvi.1998.1630.
Yoneda, M. and Maeda, K. (1989), "A study on practical estimation method for structural damping of stay cables with dampers", *Doboku Gakkai Ronbunshu*, **1989**(410), 455-458. https://doi.org/10.2208/jscej.1989.410_455.
Yoneda, M., Mochizuki, H. and Setouchi, H. (1995), "On the simplified method for estimating modal damping in stay cable with two types of dampers and its application to vibration control design", *Doboku Gakkai Ronbunshu*, **1995**(516), 183-196. https://doi.org/10.2208/jscej.1995.516-183.
Yu, Z. and Xu, Y.L. (1998), "Mitigation of three-dimensional vibration of inclined sag cable using discrete oil dampers-I. Formulation", *J. Sound Vib.*, **214**(4), 659-673. https://doi.org/10.1006/jsvi.1998.1609.
Zhou, P. and Li, H. (2016), "Modeling and control performance of a negative stiffness damper for suppressing stay cable vibrations", *Struct. Control Health Monit.*, **23**(4), 764-782. https://doi.org/10.1002/stc.1809.
Zhou, Y. and Sun, L. (2006), "Complex modal analysis of a taut cable with three-element Maxwell damper", *J. Tongji Univ.*, **34**(1), 7-12.
Zhou, H., Sun, L. and Xing, F. (2014), "Free vibration of taut cable with a damper and a spring", *Struct. Control Health Monit.*, **21**(6), 996-1014. https://doi.org/10.1002/stc.1628.

HJ

Appendix A

For the case of a spring and a viscous damper installed near the same cable support, Yoneda *et al*. (1995) proposed two simplified methods based on equivalence for estimating the combined damping effect. They are referred to as *Yoneda 1* and *Yoneda 2* respectively in the following. In the first method (*Yoneda 1*), the influence of the spring has been interpreted as reducing the effective distance between the viscous damper and the cable end. The second method considers an increment of the intrinsic stiffness of the viscous damper equivalently introduced by the spring.

Yoneda 1: The modal damping ratio is given as

$$\zeta_n \cong \frac{l_{\text{eff}}}{L}\frac{\beta_n^0 \bar{c} l_{\text{eff}}}{1+(\beta_n^0 \bar{c} l_{\text{eff}})^2} \tag{46}$$

where

$$l_{\text{eff}} = l_2 + l_3 - \frac{n\pi l_3 - L\arcsin[\phi_{k1}\sin(n\pi\, l_3/L)]}{n\pi - \arcsin[\phi_{k1}\sin(n\pi\, l_3/L)]} \tag{47}$$

Note that l_{eff} is equivalent installation length of damper, and

$$\phi_{k1} = (1.0 + P_{TK1})^{-1} \tag{48}$$

with

$$P_{TK1} = l_3(L - l_3)\, K/(LH) \tag{49}$$

Yoneda 2: The cable modal damping ratio is computed by

$$\zeta_n \cong \frac{l_2 + l_3}{L}\frac{\beta_n^0 \bar{c}(l_2 + l_3)}{[1 + k^* H^{-1}(l_2 + l_3)]^2 + [\beta_n^0 \bar{c}(l_2 + l_3)]^2} \tag{50}$$

where k^* is the equivalent stiffness parameter of damper, defined as

$$k^* = \frac{HL}{(l_2 + l_3)l_1}\frac{l_3}{(l_2 + l_3)\{H\,L/[Kl_3(l_1 + l_2)] + 1.0\} - l_3} \tag{51}$$

Appendix B

Main and Jones (2003) had given an explicit asymptotic expression for the effective damper location, and using this effective damper location, the universal curve of is generalized to account for the influence of the bushing (spring). The effective length in Eq. (46) is derived as

$$l_{\text{eff}} = (l_2 + l_3)\frac{1 + KH^{-1}l_2}{1 + KH^{-1}(l_2 + l_3)} \tag{52}$$